



Contents lists available at ScienceDirect

Archives of Biochemistry and Biophysics

journal homepage: www.elsevier.com/locate/yabbi

Microsomal glutathione transferase 1 exhibits one-third-of-the-sites-reactivity towards glutathione

Johan Ålander^{a,*}, Johan Lenggqvist^{b,1}, Peter J. Holm^c, Richard Svensson^{a,d}, Pascal Gerbaux^e, Robert H.H. van den Heuvel^f, Hans Hebert^c, William J. Griffiths^g, Richard N. Armstrong^h, Ralf Morgenstern^a

^a Institute of Environmental Medicine, Karolinska Institutet, SE-171 77 Stockholm, Sweden

^b Karolinska Biomics Center, Karolinska University Hospital, SE-171 76 Stockholm, Sweden

^c Department of Biosciences, Karolinska Institutet, SE-141 57 Huddinge, Sweden

^d DMPK & Bioanalysis, Preclinical Development, Biovitrum AB, SE-112 76 Stockholm, Sweden

^e Laboratory of Organic Chemistry, Mass Spectrometry Center, University of Mons-Hainaut, 19 Avenue Maistriau, B-7000 Mons, Belgium

^f Utrecht University, Biomolecular Mass Spectrometry, Bijvoet Center for Biomolecular Research and Utrecht Institute for Pharmaceutical Sciences, Sorbonnelaan 16, 3584 CA Utrecht, The Netherlands

^g Institute of Mass Spectrometry, School of Medicine, Room 352 Grove Building, Swansea University, Singleton Park, Swansea SA2 8PP, United Kingdom

^h Department of Biochemistry, Vanderbilt University School of Medicine, Nashville, TN 37232-0146, USA

ARTICLE INFO

Article history:

Received 13 February 2009

and in revised form 8 April 2009

Available online 3 May 2009

Keywords:

GSH

MGST1

MAPEG

Alternating sites

Cooperativity

Glutathione transferase

ABSTRACT

The trimeric membrane protein microsomal glutathione transferase 1 (MGST1) possesses glutathione transferase and peroxidase activity. Previous data indicated one active site/trimer whereas structural data suggests three GSH-binding sites. Here we have determined ligand interactions of MGST1 by several techniques. Nano-electrospray mass spectrometry of native MGST1 revealed binding of three GSH molecules/trimer and equilibrium dialysis showed three product molecules/trimer ($K_d = 320 \pm 50 \mu\text{M}$). All three product molecules could be competed out with GSH. Reinvestigation of GSH-binding showed one high affinity site per trimer, consistent with earlier data. Using single turnover stopped flow kinetic measurements, K_d could be determined for a low affinity GSH-binding site ($2.5 \pm 0.5 \text{ mM}$). Thus we can reconcile previous observations and show here that MGST1 contains three active sites with different affinities for GSH and that only the high affinity site is catalytically competent.

© 2009 Elsevier Inc. All rights reserved.

Glutathione transferases (GSTs², EC 2.5.1.18) exist as both soluble and membrane bound enzymes providing an important defence against electrophilic compounds [1]. Microsomal glutathione transferase 1 (MGST1) is a 17.3 kDa/subunit homo-trimeric enzyme [2–5] that belongs to the membrane associated proteins in eicosanoid and glutathione metabolism (MAPEG) super-family, together with MGST2 and 3, microsomal prostaglandin E synthase-1 (MPGES1), leukotriene C₄ synthase (LTC₄S) and 5-lipoxygenase activating protein (FLAP) [6]. A general theme of these proteins is the conversion of reactive compounds derived from the oxidation of lipids resulting in the protection against oxidative stress or the specific formation of highly potent lipid mediators (prostaglandins and leukotrienes). MGST1, heterologously expressed in MCF7 cells, was

shown to protect against oxidative stress [7] and several cytostatic drugs [8] whereas MPGES1 has been demonstrated to be important in the pathophysiology of fever, pain and inflammation [9–12] in mouse knock-outs.

Recently, the structures of four MAPEG membrane proteins were solved confirming the trimeric arrangement of identical subunits [4,13–16] previously demonstrated by hydrodynamic and cross-linking experiments [17,18]. The active sites are situated between subunits suggesting that each trimeric enzyme should harbour three catalytic sites. This observation contrasts with earlier data on MGST1 where binding studies by equilibrium dialysis revealed one bound glutathione (GSH) per MGST1 trimer, with a K_d of 20 μM [19]. Furthermore, pre-steady state kinetic experiments suggest the formation of one GSH thiolate anion (the catalytically competent form of GSH) and one GS⁻-trinitrobenzene Meisenheimer dead-end complex per trimer. Active site titrations revealed one active site per trimer as well [20,21]. Taken together these data point to a third-of-the-sites mechanism that most likely reflects a heterogeneous behaviour of the individual subunits. In contrast, H/D exchange experiments favours global conformational alterations upon GSH-binding [2,22] and the recently solved structure [4] actually revealed

* Corresponding author. Fax: +46 8 343849.

E-mail addresses: johan.alander@ki.se, johan.alander@live.se (J. Ålander).

¹ These two authors are contributed equally to this work.

² Abbreviations used: CDNB, 1-chloro-2,4-dinitrobenzene; GSDNB, 1-S-glutathionyl-2,4-dinitrobenzene; GSH, glutathione; GS⁻, glutathione thiolate anion; GSOH, glutathione sulfenic acid; GS₃⁻, glutathione sulphonate; GST, glutathione transferase; MAPEG, membrane associated proteins in eicosanoid and glutathione metabolism; MGST1, microsomal glutathione transferase 1.

three bound GSH molecules per trimer, although the resolution limit did not permit modelling of the exact interactions.

Earlier we were able to perform a mass spectrometric analysis of intact MGST1 confirming the oligomeric structure and establishing that this technique was applicable to a membrane protein [23]. Technological improvements in the form of an automated nano-electrospray method capable of high spray stability in the analysis of non-covalent complexes has now allowed us to study MGST1 ligand interactions by this technique demonstrating three bound GSH molecules per trimer. Thus, there is an apparent discrepancy between the experimentally determined binding stoichiometry in equilibrium dialysis, mass spectrometry data and stopped flow analysis versus H/D exchange and the solved structure.

Here we have adopted several techniques (equilibrium dialysis binding/competition with GSH and the 1-chloro-2,4-dinitrobenzene (CDNB) product 1-S-glutathionyl-2,4-dinitrobenzene (GSDNB), inhibition experiments with GSDNB, as well as single turnover experiments) to address this discrepancy. Our results show that three GSH molecules bind to each MGST1 trimer albeit with widely varying affinities (20 μM –2.5 mM). The GSH molecule in the catalytically competent thiolate anion form shows the highest affinity. A complex product inhibition pattern supports subunit cooperativity that is required for one-third-of-the-sites-reactivity.

These studies define the number of active sites in the MGST1 trimer and support an alternating one-third-of-the-sites catalytic model.

Materials and methods

Synthesis of 1-S-glutathionyl-2,4-dinitrobenzene (GSDNB)

Synthesis of GSDNB was essentially performed as described in [22].

Enzyme preparation

MGST1 was purified from male Sprague–Dawley rat livers as described previously [24], with the exception that 0.2% Triton X-100 was used during the last purification step. Enzyme concentration was determined according to Peterson [25] with bovine serum albumin as standard.

Nano-electrospray mass spectrometry

The buffer of the purified MGST1 enzyme was rapidly exchanged using Biospin p6 columns (BioRad, Hercules, CA, USA) into 50 mM ammonium acetate, pH 6.7, and test compounds (i.e., 0.1 mM reduced GSH, M_r 307.33) or GSH and glutathione sulphate (GSO_3^- , M_r 355.33) were added equimolar (0.1 mM of each) prior to analysis. In order to exclude that binding resulted from simple ionic interactions between the positively charged protein and the negatively charged ligands, L-glutamate (1 mM) was tested and found not to bind.

Nano-electrospray mass spectrometry analyses were performed on an orthogonal time-of-flight instrument (LCT, Waters Corp. Milford, MA, USA) fitted with a NanoMate source (Advion BioSystems Inc., Ithaca, NY, USA).

Spray parameters included a source temperature of 80 °C, nebuliser gas flow rate 100 L/h, cone voltage 130 V (for the GSH + GSO_3^- experiment the cone voltage was subsequently increased to 180 V to achieve best desolvation). To achieve optimum desolvation efficiency, the pressures in the interface region were optimised for each case (i.e., GSH alone and GSH + GSO_3^-) by reducing the pumping efficiency of the rotary pump by adjusting a specifically fitted speedy-valve. Vacuum readings on the first

Pirani gauge (located in the line between the source and the rotary pump) were 6.1 and 4.3 mbar, respectively. It should be noted that both samples were also analysed using identical instrument settings. In this analysis the observed stoichiometry of enzyme–ligand complexes were the same as those found under the optimised parameter settings.

The data were analysed using the manufacturer supplied MassLynx 4.0 software package. Mass spectra are shown after minimal smoothing ($3 \times$ Savitsky Golay smoothing, smooth window 5 channels). For calculation of mass increase, the centroids of the ion envelopes were determined using 30% of the peak top and a minimum peak-width at half-height of 10 channels.

Equilibrium dialysis with GSDNB

Buffer exchange and removal of GSH from the purified enzyme were performed by two gel filtrations, first in buffer A (10 mM K-P_i, 20% glycerol, 0.2% Triton X-100, 0.1 mM EDTA, pH 7.0), second in Eq-buffer (0.1 M KCl, 10 mM K-P_i, 20% glycerol, 0.2% Triton X-100, 0.1 mM EDTA, pH 8.0) on 10 DG columns (BioRad Laboratories) according to the manufacturer's instructions. The GSH free enzyme was mixed with GSDNB at concentrations varying from 50 to 1000 μM , and the mixture was dispensed into one half of the dialysis cell [19] while the other half was filled with Eq-buffer containing an equivalent amount of GSDNB. Following agitation at 4 °C overnight, the concentrations of GSDNB from both halves of the dialysis cell were measured spectrophotometrically on a Philips PU8720 UV/VIS at 340 nm ($\epsilon_{340} = 9600 \text{ M}^{-1} \text{ cm}^{-1}$). A 0.3 cm cuvette was used when the GSDNB concentration exceeded 300 μM . The dialysis membrane used (Spectrum Spectra/Por®, molecular weight cut-off of 12–14,000 Da) was prepared according to the manufacturers instructions.

Equilibrium dialysis with GSH

Buffer exchange and removal of GSH from the purified enzyme were performed by two gel filtrations, first in Eq-buffer, second in buffer X (0.1 M K-P_i, 20% glycerol, 0.2% Triton X-100, 0.1 mM EDTA, pH 7.0) containing 10 mM β -mercapthoethanol on 10 DG columns. The GSH free enzyme was mixed with pH-adjusted GSH at concentrations varying from 5 to 1000 μM containing 0.3 μCi ^{35}S -labelled GSH (PerkinElmer, USA), and the mixture was dispensed into one half of the dialysis cell [19] while the other half was filled with buffer X containing an equivalent amount of GSH. Following agitation at 4 °C overnight, the concentrations of GSH from both halves of the dialysis cell were measured on a Beckman LS 5000CE beta scintillation counter. The dialysis membrane used was prepared as for the GSDNB dialysis.

Determination of K_d and B_{max}

Determination of K_d and B_{max} were performed with the software GraphPad Prism 4 using a one site binding hyperbolic equation (Eq. (1)). Measurement values are given \pm standard error of the mean. Outliers were statistically rejected with Grubbs' test as described in the GraphPad Prism Statistical Handbook.

$$[E \cdot L]_{eq} = \frac{[E]_0 [L]_{eq}}{K_d + [L]_{eq}} \quad (1)$$

where L = GSH or GSDNB, respectively.

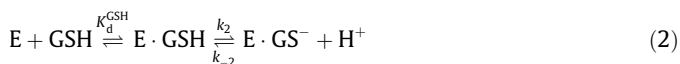
Equilibrium dialysis with GSDNB and GSH

Buffer exchange and removal of GSH from the purified enzyme, dialysis membrane used and measurement of GSDNB concentra-

tion were done as for equilibrium dialysis with GSDNB. The GSH free enzyme was mixed with 800 μM GSDNB and pH-adjusted GSH at concentrations varying from 0 to 50 mM. In a control experiment the amount of reduced GSH was measured on the enzyme free side of the dialysis membrane using 5,5'-dithio-bis(2-nitrobenzoic acid) in a 0.2 M potassium phosphate buffer, pH 8.0 ($\epsilon_{412} = 13,600 \text{ M}^{-1} \text{ cm}^{-1}$). A part of GSDNB became irreversibly bound ($\approx 20\%$ of the monomer, as determined by lack of displacement with the strong inhibitor GSO_3^-) and GSH became partly oxidised at low concentrations ($< 1 \text{ mM}$). The oxidation of GSH did not exceed 70% and was corrected for.

Stopped flow kinetics

Purified enzyme was gel filtered on 10 DG columns in buffer X containing 0.1 mM GSH. Active site titration was performed by mixing the enzyme containing pH-adjusted GSH with CDNB in buffer X (0.75 mM and 0.05 mM, respectively, final concentrations), on an Applied Photophysics stopped-flow instrument at 340 nm ($\epsilon_{340} = 9600 \text{ M}^{-1} \text{ cm}^{-1}$) and 5 °C. Thiolate anion formation after a single turnover was measured on the same instrument at 240 nm ($\epsilon_{240} = 5000 \text{ M}^{-1} \text{ cm}^{-1}$) and 5 °C at GSH concentrations ranging from 0.5 to 16 mM using 17 μM CDNB (equimolar to the enzyme active site concentration), final concentrations. Determination of K_d , k_2 and k_{-2} (Eqs. (2) and (3)) was performed with the software GraphPad Prism 4 and measurement values are given \pm standard error of the mean.



$$k_{\text{obs}} = k_{-2} + \frac{k_2[\text{GSH}]}{K_d^{\text{GSH}} + [\text{GSH}]} \quad (3)$$

Inhibition studies with GSDNB

The enzyme activity was determined in 0.1 M potassium phosphate buffer, pH 6.5, containing 0.1% Triton X-100 on a Philips PU8720 UV/VIS spectrophotometer at 340 nm with CDNB. Determination of K_m and k_{cat} were made with the software GraphPad Prism 4 using non-linear regression. To visualise inhibition type, Lineweaver-Burk plots were used. Superimposed lines in Lineweaver-Burk plots were made using K_m and k_{cat} values obtained from non-linear regression fits. Values are given \pm standard error of the mean.

Results

Non-covalent mass spectrometry to determine GSH-binding stoichiometry

Electrospray analysis of the MGST1 sample (with 0.1 mM GSH) showed a mass spectrum dominated by detergent clusters in the m/z range < 1500 (Fig. 1A). However, ions corresponding to the enzyme were observed in the high mass range (shown in 36-fold magnification in Fig. 1A). Two separate charge state envelopes are observed corresponding to the monomeric and trimeric forms of the enzyme (as indicated by M and T in Fig. 1A). The most abundant trimeric species observed was that containing three GSH molecules, while under the conditions used only a minor portion is observed that contains two GSH molecules (c.f. Fig. 1C).

Upon co-addition of an equivalent amount (0.1 mM) of GSO_3^- to the enzyme-GSH solution, full competition by the inhibitor is observed. In Fig. 1B and C are shown the overlaid spectra from the analysis of MGST1 with 0.1 mM GSH and GSH + GSO_3^- . In B is shown the 8+ monomeric charge state and in C the 14+ trimeric charge state. As can be seen the addition of inhibitor does not alter

the mass for the monomeric form. Indeed, in Fig. 1B, the two peaks observed in the spectrum correspond to the non-acetylated, m/z 2169.3 and the *N*-acetylated enzyme, m/z 2174.5 [26]. On the other hand, for the trimer species, a mass increase is observed as exemplified in Fig. 1C where the most abundant peak of the 14+ charge state is shifted from m/z 3790.1 to 3800.0. The average mass shift (calculated from the three most abundant trimer charge states, 13+, 14+ and 15+) observed was 141.53 Da. The error compared to the theoretical mass shift ($355.33 - 307.33 = 48 \text{ Da}$, $3 \times 48 = 144 \text{ Da}$) was 2.47 Da. This corresponds to a mass shift error of $\sim 47 \text{ ppm}$ for the entire (three times GSH bound) trimeric enzyme. Together, this strongly suggests complete exchange of all three GSH molecules for three inhibitor molecules.

Re-evaluation of GSH-binding affinity and stoichiometry by equilibrium dialysis

In order to re-evaluate our previous binding data we repeated equilibrium dialysis experiments with ^{35}S -labelled GSH as described in [19], with the exception that 10 mM β -mercaptoethanol was used as a reducing agent instead of 0.1 M DTT. With the enzyme concentration used (29–31 μM trimer corresponding to $\approx 90 \mu\text{M}$ potential binding sites), we could only observe one GSH bound per trimer ($B_{\text{max}} 0.85 \pm 0.03$, $K_d 16 \pm 4 \mu\text{M}$, Eq. (1) and Fig. 2), confirming our previous results [19]. We therefore suggest that MGST1 harbours one high affinity and two low affinity sites for GSH. In this case K_d and B_{max} most likely reflect binding of GSH to the high affinity site where the thiolate anion is stabilized. It should be noted that the measurements also put a lower limit on the K_d of the two low affinity sites (at about 400 μM). The two weaker sites could not be quantified due to practical limits in the amount of enzyme that could be used.

Determination of the binding affinity and stoichiometry of GSDNB by equilibrium dialysis

To evaluate product binding, equilibrium dialysis studies were performed utilising GSDNB. When the data were fitted to a one site binding hyperbola (Eq. (1) and Fig. 3), B_{max} was determined to 3.6 ± 0.3 product molecules per trimer, and K_d to $320 \pm 50 \mu\text{M}$. This clearly shows three active-binding sites per trimer. Attempts to fit data to a two or a three site-binding equation did not improve the fit.

Qualitative determination of GSDNB/GSH-binding competition by equilibrium dialysis

The presence of three binding sites/trimer for the product GSDNB allowed us to investigate whether GSH could compete for all three sites, which was indeed the case (Fig. 4). In principle these data could be used to determine the separate binding affinities of all three GSH molecules. However, the precision of the data is not sufficient for this purpose and only a qualitative determination could be made, indicating complete exchange at a few mM GSH. It should be noted that under these dialysis conditions GSDNB also becomes irreversibly bound to a fraction of the enzyme (approximately 20% of the monomer), as determined by lack of competition by an excess of the strong inhibitor, glutathione sulphonate (not shown).

Determination of the affinity of the third GSH molecule by stopped flow single turn over experiments

The pre-steady state kinetic properties of MGST1 [20,21] allows the performance of single turn-over experiments where the enzyme, equilibrated with various concentrations of GSH, is rapidly

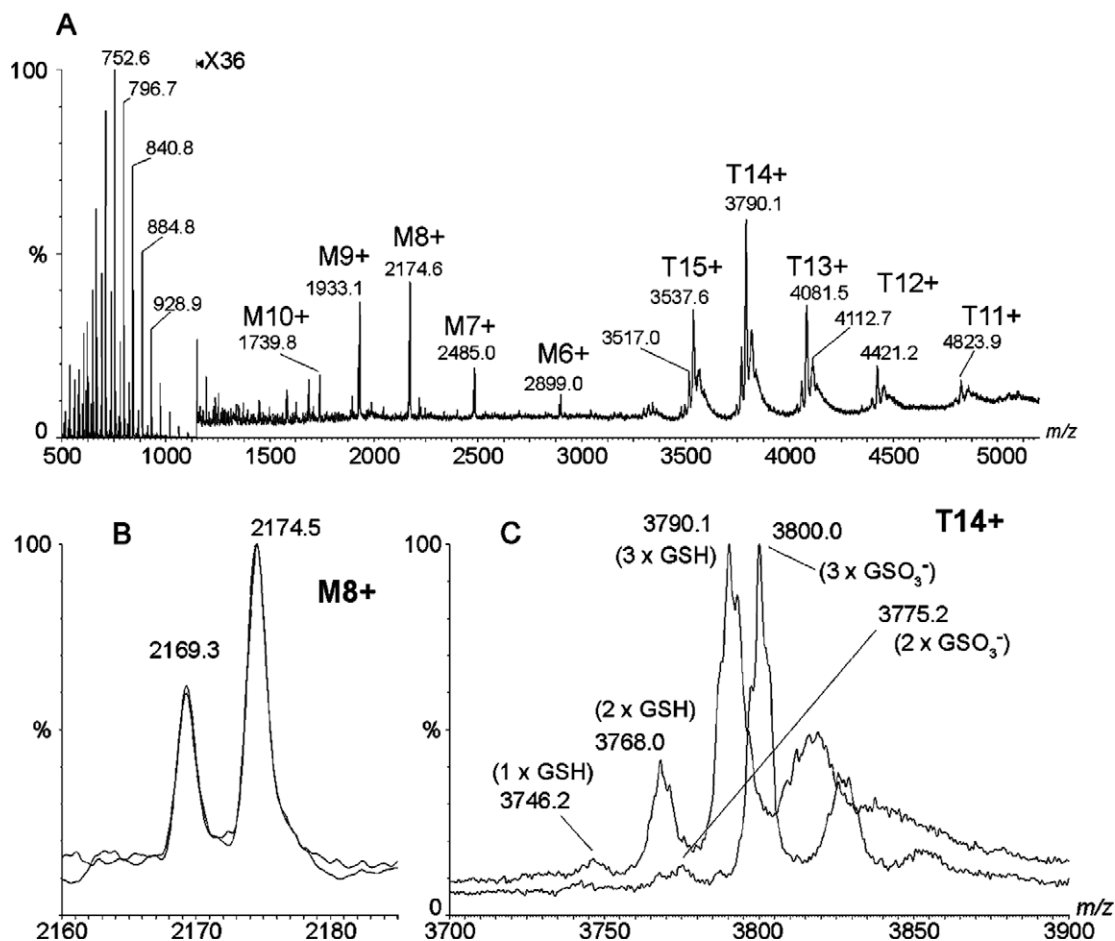


Fig. 1. MGST1 binds three GSH molecules per trimer. Automated nano-electrospray mass spectrometry analysis of MGST1–substrate/inhibitor complexes. In A is shown the full mass range (m/z 500–5000) for the analysis of detergent solubilised MGST1 in the presence of 0.1 mM GSH. Monomeric and trimeric enzyme forms are indicated by M and T, respectively. In B is shown the overlaid spectra of the 8+ monomeric charge state of MGST1 in the presence of 0.1 mM GSH alone and with equimolar amounts of GSH/GSO₃⁻. In C is shown the same spectra as in B for the m/z range of the most abundant trimeric charge state. Peaks corresponding to the binding of substrate/inhibitor molecules are indicated.

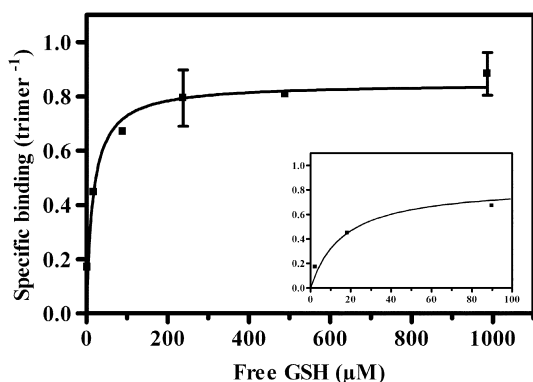


Fig. 2. Binding of GSH to MGST1 analysed by equilibrium dialysis. GSH-free MGST1 was mixed with varying ³⁵S-GSH concentrations (5–1000 µM) as described in Experimental procedures. After equilibration overnight the partitioning of GSH was measured by scintillation counting and the data were fitted to a one site binding hyperbolic equation. Enzyme concentrations varied between 29 and 31 µM trimer in different experiments ($n = 3$). The insert shows a magnification of the plot for clarity.

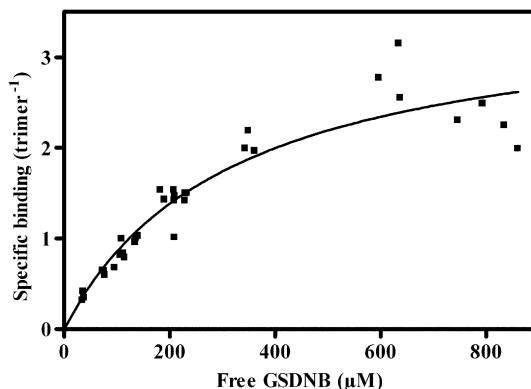


Fig. 3. Binding of the product GSDNB to MGST1 analysed by equilibrium dialysis. GSH-free MGST1 was mixed with varying GSDNB concentrations (50–1000 µM) as described in Experimental procedures. After equilibration overnight the partitioning of GSDNB was measured spectrophotometrically and the data were fitted to a one site binding hyperbolic equation. Enzyme concentrations varied between 26 and 35 µM trimer in different experiments. Each point represents a separate experiment.

mixed with a stoichiometric (1/trimer) concentration of CDNB. Upon mixing a rapid burst of product formation and release takes place. Subsequent GSH rebinding to the empty site and slow thio-

late anion formation can then be observed (the rebinding phase is shown in Fig. 5A). Fitting the GSH dependence of k_{obs} for the thio-

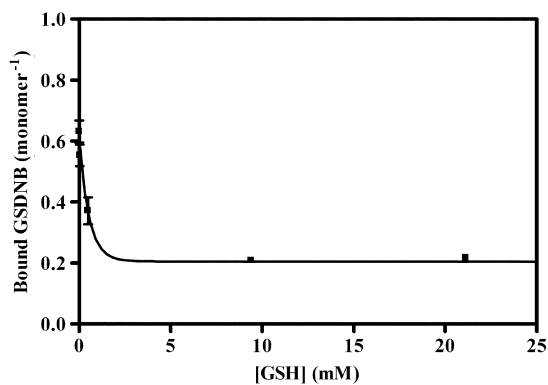


Fig. 4. GSH competition experiment against MGST1-bound GSDNB. GSH-free MGST1 was mixed with varying GSH concentration (0–22 mM) and 800 μ M GSDNB as described in Experimental procedures. After equilibration overnight the partitioning of GSDNB was measured spectrophotometrically. Enzyme concentrations varied between 17 and 23 μ M trimer in different experiments ($n = 6$).

GSH (2.5 ± 0.5 mM). The presence of a low affinity site for GSH is consistent with the mass spectrometry and structural data, and was outside the sensitivity range for detection by conventional equilibrium binding techniques.

Inhibition by GSDNB reveals a complex behaviour consistent with subunit interactions

The product GSDNB appeared to act as a mixed inhibitor towards GSH upon inspection of Lineweaver-Burk plots (Fig. 6A). However, at closer examination the inhibition pattern appears more complex as the lines do not intersect at a common point. This also became evident when non-linear regression analysis of the data was performed. Fitting a mixed inhibition model did not yield a global fit (Fig. 6B). This indicates a more complex inhibition pattern that would be consistent with cross talk between the subunits. Pure non-competitive or competitive inhibition models resulted in inferior fits (not shown).

Discussion

The members of the MAPEG superfamily are homo-trimeric integral membrane proteins. The structural data for these proteins show three active/binding sites per trimer [4,13–16] but data on MGST1 demonstrates one-third-of-the-sites-reactivity

with a single high affinity binding site for GSH [19–21]. Whether this property is common to all MAPEG proteins remain to be determined.

For the structure determination of MGST1 perfect threefold symmetry was imposed either by the crystallographic threefold axis in the P6 crystals or by applying non-crystallographic symmetry for the orthorhombic P22₁2₁ crystal form [4]. At higher resolution at least the latter may allow for detecting structural difference between monomers in the trimer provided that it follows the crystal packing. Already the observation that this crystal form is common for MGST1 as well as for MPGES1 [16] is an indication that perfect threefold symmetry may be broken, and that the individual monomers within a trimer may adopt different conformations.

Here we have examined whether the seemingly conflicting information on GSH-binding to MGST1 can be reconciled. By use of novel advances in native membrane protein–ligand interaction analysis by mass spectrometry, together with traditional binding/inhibition studies and single turn-over measurements, we have been able to give a more complete and consistent description of ligand binding to MGST1.

Automated nano-electrospray approach provided two distinct improvements compared to earlier work using glass capillary needles [23]. The nano-electrospray was more readily started and showed increased spray stability for the analysis of non-covalent complexes, as previously observed [27]. These improvements were absolutely crucial to obtain the sensitivity required. The observation of three GSH molecules bound per trimer confirms the structural data (Fig. 1C). The MGST1 monomer was not capable of binding GSH under the same conditions (Fig. 1B). This observation is consistent with the GSH-binding sites residing at the subunit interfaces [4]. Equimolar glutathione sulphonate could compete out all GSH molecules in the trimer and showed almost full occupancy which is consistent with stronger binding observed earlier [19].

We then reinvestigated our data on GSH-binding using equilibrium dialysis and observed one high affinity site ($K_d = 16$ μ M, Fig. 2) confirming previous results [19]. It should be noted that this GSH must be in the thiolate anion form (as shown earlier by active site titration experiments [20,21]).

Equilibrium dialysis with the product GSDNB revealed that three molecules bind per MGST1 trimer with modest affinity ($K_d = 320$ μ M, Fig. 3). This affinity is not much higher than with the corresponding substrate CDNB (0.5 mM [20]) indicating that the GSH molecule itself does not display tight binding in the non-thiolate form.

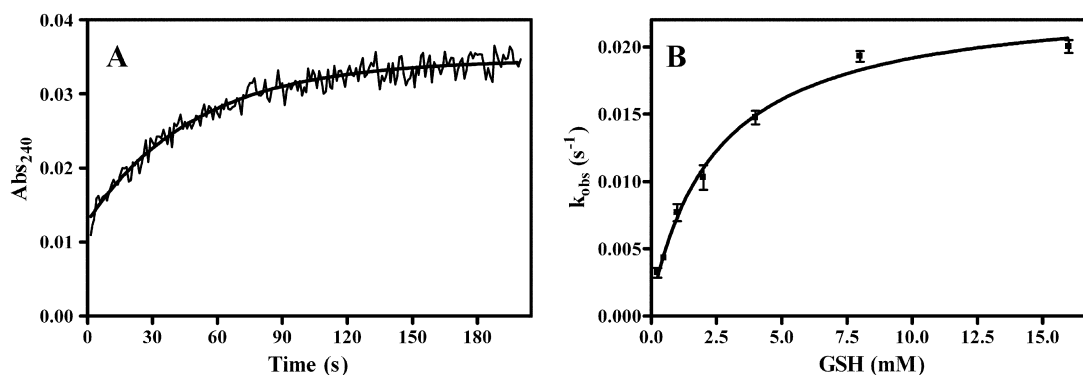


Fig. 5. GSH-binding to MGST1 that already has two GSH molecules bound. Single turnover experiment where GSH-bound MGST1 is rapidly mixed with CDNB at a ratio of 1/ trimer. Thiolate anion re-formation was recorded after the initial burst (17 μ M CDNB vs. 14 μ M MGST1-trimer). (A) The increase in absorbance at 240 nm at 16 mM GSH after mixing the enzyme with 17 μ M CDNB. The solid line is the best fit to a single exponential to obtain k_{obs} . (B) The dependence of k_{obs} for GSH thiolate formation on GSH concentration was fitted to Eq. (3) ($n = 2$ at low GSH concentrations, $n = 3$ at 8 and 16 mM). Enzyme concentration used was 14 μ M trimer as measured by an active site titration (not shown).

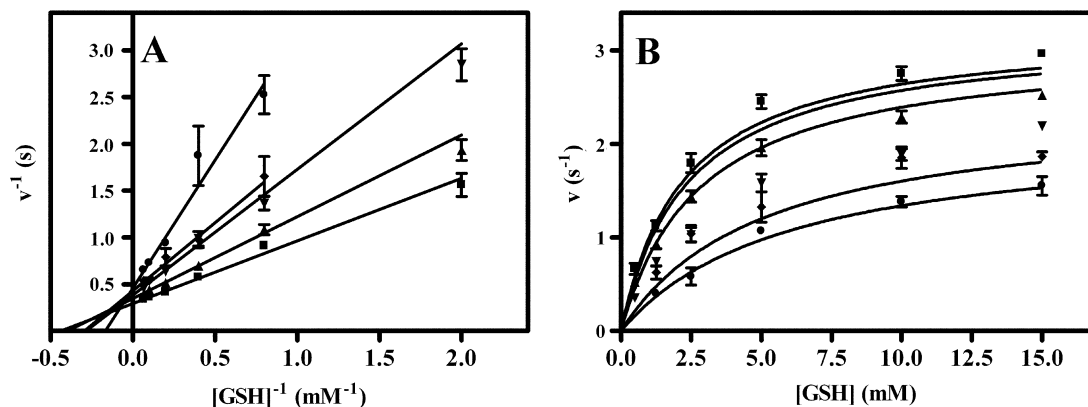


Fig. 6. Inhibition of MGST1 by the product GSDNB. Lineweaver-Burk plot (A) and a fit of the data (B) to a mixed inhibition mechanism. The concentration of GSDNB was 0 (■), 20 (▲), 80 (▼), 500 (◆) and 750 (●) μM , GSH was varied between 0.5 and 15 mM and the CDNB concentration was fixed at 0.5 mM. The enzyme concentration was 0.5 μM trimer ($n = 3$).

In order to determine the affinity for the remaining two GSH molecules we first attempted equilibrium dialysis competition experiments, using GSDNB as a probe for GSH-binding. Indeed, a high GSH concentration (of a few mM) was required to compete out all GSDNB molecules (except a low percentage that became irreversibly bound (Fig. 4)). This independently demonstrates the capacity of the enzyme to bind three GSH molecules as expected. Although, in principle, the competition data could reveal the binding affinities for all three GSH molecules, the data lack the precision necessary to do so. The lack of precision is principally due to the limit on protein concentrations that can be achieved.

In order to determine the affinity of the third GSH molecule a different strategy was therefore employed, using single turn-over experiments. In essence this experiment involves removing one (of three) GSH molecule from the MGST1 trimer and observe as a new GSH binds and forms the thiolate. GSH thiolate formation is a two step process known to proceed via rapid equilibrium binding of GSH followed by a slow de-protonation of GSH [20,21]. Analysis of the GSH concentration behaviour allows determination of the K_d for the third GSH molecule (shown to be 2.5 mM, Fig. 5A). Thus one of the low affinity sites is defined. The K_d for the “second” GSH remains undetermined but we speculate that the value lies between 0.4 and 2.5 mM. This assumption is based on the high occupancy during mass spectrometry (Fig. 1A and C) and the weak, but single affinity, binding of the product GSDNB (Fig. 3). It is interesting to note that the K_d of 50 mM for GSH, obtained from binding to the empty enzyme [20], is much larger than the K_d of 2.5 mM measured for the dissociation of the third GSH obtained here. Thus, enzyme that has already bound GSH in one or two of the three sites binds additional GSH more strongly.

In principle, one-third-of-the-sites-reactivity lowers the capacity of MGST1 and as a consequence might not be favoured by evolution. The membrane location of MGST1, however, poses specific challenges that can provide a rationale for the observed mechanism. The enzyme serves to link hydrophilic GSH to hydrophobic substrates that are dissolved in the surrounding membrane [28]. Positioning GS^- deep in the enzyme for optimal access to membrane substrates, together with subsequent release of product to the cytosol, requires considerable structural transitions by the protein. By coupling these structural transitions to the ability to form tightly bound thiolate anion, the enzyme can achieve selectivity and thereby avoid becoming trapped with a tightly bound product. This is a realistic scenario given the enormous structural diversity of electrophilic substrates that MGST1 is capable of using [28,29]. By having a low affinity for protonated GSH the enzyme also avoids becoming trapped in the GSH sulfenic acid form (GSOH), a product

of the peroxidase activity of MGST1. Although the suggested mechanism could operate at each site independently, the stabilisation of one GS^- on a neighbouring subunit may promote structural transitions, leading to product release. We believe that this is the key principle that explains one-third-of-sites-reactivity. In fact, we have observed that several hydrophobic ligands can increase the enzyme activity, consistent with the latter suggestion [30]. The dynamics of protonation/deprotonation between the individual subunits is not known, and, if influenced by second substrate binding, could also direct efficient catalysis.

To summarise, GSH initially binds to each of the three low affinity sites in MGST1 ($K_d = 50$ mM). Once one molecule of bound GSH is deprotonated ($K_d = 20$ μM), the remaining active sites bind their GSH more strongly ($K_d = 2.5$ mM for the third GSH), but cannot promote deprotonation. This results in one-third-of-sites-reactivity.

Acknowledgments

We thank Peter Lachmann, Stockholm University, for the help with the stopped flow apparatus. This work was supported by the Swedish Research Council, Vinnova (Swedish Governmental Agency for Innovation Systems), JST (Japan Science and Technology Agency), the National Institutes of Health Grant R01 GM030910, the Swedish Cancer Society, the foundation Lars Hiertas Minne, the Swedish Foundation for Medical Research (SSMF) and Funds from Karolinska Institutet. P.G. (FRS-FNRS Research associate) thanks the FRS-FNRS and the University of Mons-Hainaut for financial support. We also thank the reviewers for their insightful comments.

References

- [1] R. Rinaldi, E. Eliasson, S. Swedmark, R. Morgenstern, *Drug Metab. Dispos.* 30 (2002) 1053–1058.
- [2] L.S. Busenlehner, S.G. Codreanu, P.J. Holm, P. Bhakat, H. Hebert, R. Morgenstern, R.N. Armstrong, *Biochemistry* 43 (2004) 11145–11152.
- [3] H. Hebert, I. Schmidt-Krey, R. Morgenstern, K. Murata, T. Hirai, K. Mitsuoka, Y. Fujiyoshi, *J. Mol. Biol.* 271 (1997) 751–758.
- [4] P.J. Holm, P. Bhakat, C. Jegerschöld, N. Gyobu, K. Mitsuoka, Y. Fujiyoshi, R. Morgenstern, H. Hebert, *J. Mol. Biol.* 360 (2006) 934–945.
- [5] P.J. Holm, R. Morgenstern, H. Hebert, *Biochim. Biophys. Acta* 1594 (2002) 276–285.
- [6] P.J. Jakobsson, R. Morgenstern, J. Mancini, A. Ford-Hutchinson, B. Persson, *Protein Sci.* 8 (1999) 689–692.
- [7] A. Siritantikorn, K. Johansson, K. Åhlen, R. Rinaldi, T. Suthiphongchai, P. Wilairat, R. Morgenstern, *Biochem. Biophys. Res. Commun.* 355 (2007) 592–596.
- [8] K. Johansson, K. Åhlen, R. Rinaldi, K. Sahlander, A. Siritantikorn, R. Morgenstern, *Carcinogenesis* 28 (2007) 465–470.

- [9] D. Engblom, S. Saha, L. Engström, M. Westman, L.P. Audoly, P.J. Jakobsson, A. Blomqvist, *Nat. Neurosci.* 6 (2003) 1137–1138.
- [10] T. Mabuchi, H. Kojima, T. Abe, K. Takagi, M. Sakurai, Y. Ohmiya, S. Uematsu, S. Akira, K. Watanabe, S. Ito, *Neuroreport* 15 (2004) 1395–1398.
- [11] S. Saha, L. Engström, L. Mackerlova, P.J. Jakobsson, A. Blomqvist, *Am. J. Physiol. Regul. Integr. Comp. Physiol.* 288 (2005) R1100–R1107.
- [12] C.E. Trebino, J.L. Stock, C.P. Gibbons, B.M. Naiman, T.S. Wachtmann, J.P. Umland, K. Pandher, J.M. Lapointe, S. Saha, M.L. Roach, D. Carter, N.A. Thomas, B.A. Durtschi, J.D. McNeish, J.E. Hambor, P.J. Jakobsson, T.J. Carty, J.R. Perez, L.P. Audoly, *Proc. Natl. Acad. Sci. USA* 100 (2003) 9044–9049.
- [13] H. Ago, Y. Kanaoka, D. Irikura, B.K. Lam, T. Shimamura, K.F. Austen, M. Miyano, *Nature* 448 (2007) 609–612.
- [14] A.D. Ferguson, B.M. McKeever, S. Xu, D. Wisniewski, D.K. Miller, T.T. Yamin, R.H. Spencer, L. Chu, F. Ujjainwalla, B.R. Cunningham, J.F. Evans, J.W. Becker, *Science* 317 (2007) 510–512.
- [15] D.M. Molina, A. Wetterholm, A. Kohl, A.A. McCarthy, D. Niegowski, E. Ohlson, T. Hammarberg, S. Eshaghi, J.Z. Haeggström, P. Nordlund, *Nature* 448 (2007) 613–616.
- [16] C. Jegerschöld, S.C. Pawelzik, P. Purhonen, P. Bhakat, K.R. Gheorghe, N. Gyobu, K. Mitsuoka, R. Morgenstern, P.J. Jakobsson, H. Hebert, *Proc. Natl. Acad. Sci. USA* 105 (2008) 11110–11115.
- [17] G. Lundqvist, T. Yucel-Lindberg, R. Morgenstern, *Biochim. Biophys. Acta* 1159 (1992) 103–108.
- [18] R. Morgenstern, C. Guthenberg, J.W. Depierre, *Eur. J. Biochem.* 128 (1982) 243–248.
- [19] T.H. Sun, *Biochem. J.* 326 (Pt. 1) (1997) 193–196.
- [20] R. Morgenstern, R. Svensson, B.A. Bernat, R.N. Armstrong, *Biochemistry* 40 (2001) 3378–3384.
- [21] R. Svensson, J. Ålander, R.N. Armstrong, R. Morgenstern, *Biochemistry* 43 (2004) 8869–8877.
- [22] L.S. Busenlehner, J. Ålander, C. Jegerschöld, P.J. Holm, P. Bhakat, H. Hebert, R. Morgenstern, R.N. Armstrong, *Biochemistry* 46 (2007) 2812–2822.
- [23] J. Lengqvist, R. Svensson, E. Evergren, R. Morgenstern, W.J. Griffiths, *J. Biol. Chem.* 279 (2004) 13311–13316.
- [24] R. Morgenstern, J.W. DePierre, *Eur. J. Biochem.* 134 (1983) 591–597.
- [25] G.L. Peterson, *Anal. Biochem.* 83 (1977) 346–356.
- [26] L.J. Shore, G.B. Odell, C. Fenselau, *Biochem. Pharmacol.* 49 (1995) 181–186.
- [27] C.A. Keetch, H. Hernandez, A. Sterling, M. Baumert, M.H. Allen, C.V. Robinson, *Anal. Chem.* 75 (2003) 4937–4941.
- [28] E. Mosialou, F. Piemonte, C. Andersson, R.M. Vos, P.J. van Bladeren, R. Morgenstern, *Arch. Biochem. Biophys.* 320 (1995) 210–216.
- [29] R. Morgenstern, G. Lundqvist, V. Hancock, J.W. DePierre, *J. Biol. Chem.* 263 (1988) 6671–6675.
- [30] E. Mosialou, R. Morgenstern, *Chem. Biol. Interact.* 74 (1990) 275–280.